



Providing Choice & Value

Generic CT and MRI Contrast Agents



CONTACT REP

AJNR

This information is current as
of July 25, 2025.

Refining the Neuroimaging Definition of the Dandy-Walker Phenotype

M.T. Whitehead, M.J. Barkovich, J. Sidpra, C.A. Alves,
D.M. Mirsky, Ö. Öztekin, D. Bhattacharya, L.T. Lucato, S.
Sudhakar, A. Taranath, S. Andronikou, S.P. Prabhu, K.A.
Aldinger, P. Haldipur, K.J. Millen, A.J. Barkovich, E.
Boltshauser, W.B. Dobyns and K. Mankad

AJNR Am J Neuroradiol published online 22 September
2022

<http://www.ajnr.org/content/early/2022/09/22/ajnr.A7659>

Refining the Neuroimaging Definition of the Dandy-Walker Phenotype

M.T. Whitehead, M.J. Barkovich, J. Sidpra, C.A. Alves, D.M. Mirsky, Ö. Öztekin, D. Bhattacharya, L.T. Lucato, S. Sudhakar, A. Taranath, S. Andronikou, S.P. Prabhu, K.A. Aldinger, P. Haldipur, K.J. Millen, A.J. Barkovich, E. Boltshauser, W.B. Dobyns, and K. Mankad



ABSTRACT

BACKGROUND AND PURPOSE: The traditionally described Dandy-Walker malformation comprises a range of cerebellar and posterior fossa abnormalities with variable clinical severity. We aimed to establish updated imaging criteria for Dandy-Walker malformation on the basis of cerebellar development.

MATERIALS AND METHODS: In this multicenter study, retrospective MR imaging examinations from fetuses and children previously diagnosed with Dandy-Walker malformation or vermian hypoplasia were re-evaluated, using the choroid plexus/tela choroidea location and the fastigial recess shape to differentiate Dandy-Walker malformation from vermian hypoplasia. Multiple additional measures of the posterior fossa and cerebellum were also obtained and compared between Dandy-Walker malformation and other diagnoses.

RESULTS: Four hundred forty-six examinations were analyzed (174 fetal and 272 postnatal). The most common diagnoses were Dandy-Walker malformation (78%), vermian hypoplasia (14%), vermian hypoplasia with Blake pouch cyst (9%), and Blake pouch cyst (4%). Most measures were significant differentiators of Dandy-Walker malformation from non-Dandy-Walker malformation both pre- and postnatally ($P < .01$); the tegmentovermian and fastigial recess angles were the most significant quantitative measures. Posterior fossa perimeter and vascular injury evidence were not significant differentiators pre- or postnatally ($P > .3$). The superior posterior fossa angle, torcular location, and vermian height differentiated groups postnatally ($P < .01$), but not prenatally ($P > .07$).

CONCLUSIONS: As confirmed by objective measures, the modern Dandy-Walker malformation phenotype is best defined by inferior predominant vermian hypoplasia, an enlarged tegmentovermian angle, inferolateral displacement of the tela choroidea/choroid plexus, an obtuse fastigial recess, and an unpaired caudal lobule. Posterior fossa size and torcular location should be eliminated from the diagnostic criteria. This refined phenotype may help guide future study of the numerous etiologies and varied clinical outcomes.

ABBREVIATIONS: BPC = Blake's pouch cyst; DWM = Dandy-Walker malformation; RL = rhombic lip; TTC = taenia-tela choroidea complex; TVA = tegmentovermian angle; VH = vermian hypoplasia

The traditionally described Dandy-Walker malformation (DWM) comprises a range of structural abnormalities involving the

cerebellum and posterior cranial fossa.¹ While classic imaging features are firmly established, the inclusion and exclusion criteria used

Received April 20, 2022; accepted after revision June 28.

From the Department of Radiology (M.T.W.) and Prenatal Pediatrics Institute (M.T.W.), Children's National Hospital, Washington DC; The George Washington University School of Medicine and Health Sciences (M.T.W.), Washington DC; Division of Neuroradiology (M.T.W., C.A.A., S.A.), Children's Hospital of Philadelphia, Philadelphia, Pennsylvania; Department of Radiology, Perelman School of Medicine (M.T.W., S.A.), University of Pennsylvania, Philadelphia, Pennsylvania; Department of Radiology and Biomedical Imaging (M.J.B., A.J.B.) University of California, San Francisco, San Francisco, California; Neuroradiology Section (M.J.B., A.J.B.), University of California, San Francisco-Benioff Children's Hospital, San Francisco, California; Developmental Biology and Cancer Section (J.S., K.M.), University College London Great Ormond Street Institute of Child Health, London, UK; Department of Neuroradiology (J.S., S.S., K.M.), Great Ormond Street Hospital for Children National Health Service Foundation Trust, London, UK; Department of Radiology (D.M.M.), Children's Hospital Colorado, University of Colorado School of Medicine, Aurora, Colorado; Department of Neuroradiology (Ö.Ö.), Bakırçay University, Çi li Education and Research Hospital, Izmir, Turkey; Department of Neuroradiology (D.B.), Royal Victoria Hospital, Belfast, UK; Division of Diagnostic Neuroradiology (L.T.L.), Hospital das Clínicas da Faculdade de Medicina da Universidade de São Paulo, São Paulo, Brazil; Department of Medical Imaging (A.T.), Women's and Children's Hospital, North Adelaide, South Australia, Australia; Faculty of Medicine (A.T.), University of Adelaide, Adelaide, South Australia, Australia; Department of Neuroradiology (S.P.P.), Boston Children's Hospital, Harvard Medical School, Boston, Massachusetts; Center for Integrative Brain Research (K.A.A., P.H., K.J.M.), Seattle Children's Research Institute, Seattle, Washington; University of Washington School of Medicine (K.J.M.), Seattle, Washington; Department of Pediatric Neurology (E.B.), University Children's Hospital, Zürich, Switzerland; and Department of Genetics and Metabolism (W.B.D.), Department of Pediatrics, University of Minnesota, Minneapolis, Minnesota.

First authorship is shared between M.T. Whitehead and M.J. Barkovich, order as listed.

Please address correspondence to Matthew Whitehead, MD, Division of Neuroradiology, Children's Hospital of Philadelphia, 3401 Civic Center Blvd, Philadelphia, PA 19104; e-mail: WhiteheadM@CHOP.edu

Indicates article with online supplemental data.

<http://dx.doi.org/10.3174/ajnr.A7659>

to define less typical imaging patterns are inexact, both in theory and in practice. Indeed, though “Dandy-Walker variant,” a term that was introduced as a means of describing milder phenotypes, has been strongly discouraged due to misuse, it still appears regularly in the literature and in the clinical practice of institutions around the world.²⁻⁴ Although one could advocate abandoning the eponym altogether, we instead designate DWM as a structural phenotype as a way to succinctly define its complex-but-specific anatomic composition. DWM is indeterminant in etiology when isolated and may be acquired or genetic.^{5,6} Thus, its causes, risk factors, prognoses, and outcomes will remain enigmatic, and counseling challenges will linger until its neuroimaging phenotype is better defined and issues pertaining to classification/categorization and ascertainment bias are resolved.

Recently recognized features that can help distinguish DWM from its mimics, including the tail sign,⁷ choroid plexus/tela choroidea location,^{6,8,9} and fastigial recess shape,^{10,11} have not yet been incorporated into the diagnostic criteria. On the other hand, as we demonstrate here, posterior fossa enlargement and torcular location should probably be discarded because these are variable in and are not specific for DWM.

Using the choroid plexus/tela choroidea location and fastigial recess shape, together with conventional qualitative and quantitative cerebellar and posterior fossa measures, we retrospectively evaluated a large series of fetal and postnatal brain MRIs from children determined to have DWM at initial imaging to achieve the following: 1) refining the phenotypic imaging criteria for DWM; 2) estimating the diagnostic accuracy of historical MR imaging examinations; and, 3) using our refined criteria of DWM (tail sign, choroid plexus/tela choroidea location, and fastigial recess angle) to compare DWM and non-DWM groups with regard to conventional qualitative and quantitative cerebellar and posterior fossa measures.

MATERIALS AND METHODS

This 11-center international study was conducted after site-specific institutional review board approval. Written informed consent was waived due to the retrospective nature of the study. Institution-specific radiology information systems were searched for all fetal and postnatal pediatric (19 years of age or younger) brain MR imaging examinations with radiology reports containing the terms “Dandy-Walker” and/or “vermian hypoplasia.” An additional 21 postnatal MRIs from patients with DWM included in a previous study were also included.⁵ Examinations were manually reviewed to confirm the diagnoses. After excluding incomplete examinations, examinations with severe motion artifacts, and those without posterior fossa anomalies or malformations, each case was evaluated for the following (to the extent allowed by the technique): indication, magnet and imaging parameters, vermian size/morphology, fastigial recess angle, posterior fossa size/morphology, choroid plexus and taenia-tela choroidea complex (TTC) location, torcular location, evidence of prior injury (hemorrhage and/or encephalomalacia), brainstem abnormalities, and supratentorial findings. Specific vermian measures included the following: anterior-posterior diameter (millimeter), height (millimeter), lobe number, vermian ratio, tail sign, fastigial recess

angle, and tegmentovermian angle (TVA).^{5,7,11-17} On the basis of recent histopathologic studies of normal human vermian embryologic development, the vermian ratio was considered abnormal when the collective size of the posterior and central lobes was less than approximately twice the size of the anterior lobe using a line drawn from the fastigial point to the primary fissure (Online Supplemental Data).^{10,11}

Specific posterior fossa assessments included the following: torcular location, posterior fossa perimeter (millimeter), superior posterior fossa angle, falx cerebelli abnormalities (absent, truncated, or multiplied), and cisterna magna depth (millimeter).^{12,13,18} Given the technical and motion-related challenges inherent in fetal MR imaging, measurements were obtained on the images that best approximated conventional imaging planes. If certain measurements could not be obtained accurately in a particular case, those data were excluded. Age, sex, history of prematurity, twinning history, shunt history, and known genetic abnormalities were obtained from the medical record where available.

All cases were independently reviewed by senior neuroradiologists at each participating institution. To ensure standardization across centers, a board-certified pediatric neuroradiologist (K.M.) with 14 years of posttraining experience independently reviewed all anonymized images to verify the diagnosis, qualitative and quantitative measures, and the reporting of additional brainstem malformations. Discrepancies in qualitative and quantitative measures and the reporting of additional brainstem malformations were resolved via independent review by a third author (J.S.).

Working definitions for this study were based on literature review and group consensus (Online Supplemental Data). DWM was defined by vermian hypoplasia with an inferior severity gradient, vermian under-rotation with an increased TVA, an enlarged fourth ventricle with an obtuse fastigial recess, an unpaired caudal lobule (tail sign when visible), and inferior and/or lateral displacement of the TTC and/or the choroid plexus when visible (Figure) (Online Supplemental Data).^{6,10,11} “Vermian hypoplasia” was defined as global reduction in vermian volume without vermian ratio reduction, lobe deficit, fissural enlargement, fastigial recess angle blunting, or inferolateral TTC/choroid plexus displacement. “Inferior vermian hypoplasia” was defined as inferior-predominant vermian hypoplasia, a decreased vermian ratio with/without lobe reduction, an acute fastigial recess angle, and lack of inferolateral TTC/choroid plexus displacement (Online Supplemental Data). Blake pouch cyst (BPC) was defined by a normally sized vermis, enlarged TVA, and TTC/choroid plexus location at the inferomedial cerebellar margin (when visible). We compared the original and updated diagnoses on the basis of this classification scheme.

Imaging Technique

Sixty-eight patients (15%) were scanned at 3T (60 postnatal; 8 fetal), and the other 339 patients (173 postnatal; 166 fetal) were scanned at 1.5T. Due to the number of participating centers and the several decades of imaging included in the patient cohort, there was significant heterogeneity in terms of scanner manufacturer, sequences acquired, and imaging parameters. Minimum postnatal MR imaging sequences for inclusion were sagittal T1WI and axial T2WI, all with ≤5-mm section thicknesses. Additional sequences including T2 FLAIR, SWI, DWI/DTI, and

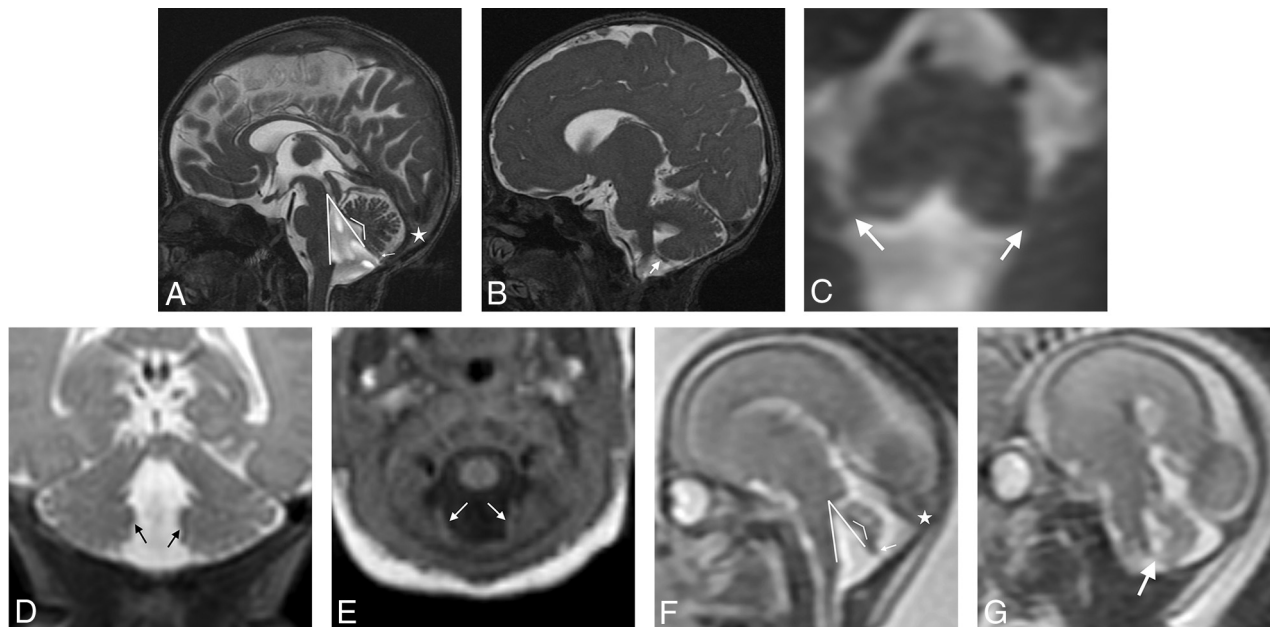


FIGURE. Dandy-Walker phenotype: MR imaging criteria. Balanced steady-state sequence (0.8-mm section thickness, 0.4-mm section spacing) in the sagittal (A), parasagittal (B), and axial (C) planes and coronal T2WI (1-mm section thickness, 0-mm section spacing, D) and axial T1WI (1-mm section thickness, 0-mm section spacing, E) from a neonate show inferior predominant VH, an enlarged tementovermian angle at 35° (*thick-lined angle*, A), an obtuse fastigial angle at 119° (*thin-lined angle*, A), an unpaired caudal lobe (ie, tail-sign; *thin arrow*, A), and inferolateral displacement of the taenia-tela choroidea complex and choroid plexus distant from the vermis (*thick arrows*, B–E). Similar findings are seen in the same patient on fetal MR imaging at 22 weeks' gestational age in sagittal (F) and parasagittal single-shot T2WI (3-mm section thickness, 0-mm section spacing, G). Note a normal torcular position (*stars*); the torcular position is variable in all forms of posterior fossa abnormalities/anomalies and should not be considered in isolation as an interpretive criterion in the differential diagnosis.

gradient recalled-echo were reviewed in most cases (when available). Multiplanar single-shot FSE/TSE sequences with section thickness ranging from 2 to 5 mm were acquired in all fetal MR imaging examinations.

Statistical Analysis

The Mann-Whitney *U* test was performed to evaluate differences in continuous variables between the DWM and non-DWM groups. The χ^2 test was used for categoric variables. Receiver operating characteristic curves and concordance statistics comparing the DWM and non-DWM groups were generated for the continuous variables in both the prenatal and postnatal groups. An optimized linear model for discriminating DWM from non-DWM groups was created by the stepwise Akaike information criterion optimization in both the prenatal and postnatal cohorts. Receiver operating characteristic curves and concordance statistics were generated for both the empirically generated and stepwise Akaike information criterion-optimized linear models. Missing data were encountered at random, and corresponding patients were discarded from subsequent, associated statistical analyses. Statistical analyses were performed using R Version 4.1.1 (<http://www.r-project.org/>) and approved by a consulting statistician.

RESULTS

Four hundred seventy-six brain MR imaging examinations were evaluated. Thirty examinations were excluded due to insufficient image quality and/or deficient data, leaving 446 examinations (fetal: *n* = 174, 39.0%; median gestational age/interquartile

range/range = 21.9 weeks/6.2 weeks/17–39 weeks, male/female = 1:1.0; postnatal: *n* = 272 [61.0%]; median age/interquartile range = 190 days/1472 days, male/female = 1:1.2) from 407 patients. Thirty-nine patients were imaged both prenatally and postnatally. Of these, 9 (23.1%) diagnoses were revised postnatally though no single diagnosis was significantly affected. Most patients had either DWM (78%, *n* = 329) (Online Supplemental Data) or vermian hypoplasia (VH; 13.9%, *n* = 62) (Online Supplemental Data) as would be expected on the basis of the method of case acquisition. However, a minority of cases were re-classified as either BPS (*n* = 16, 3.6%) or concurrent VH and BPC (*n* = 39, 8.7%) (Online Supplemental Data).

Seventy-five percent (*n* = 129) of fetal MR imaging cases and 73% (*n* = 200) of postnatal examinations had DWM. The remaining were diagnosed with VH (fetal: *n* = 12, 6.9%; postnatal: *n* = 50, 18.3%), BPC (fetal: *n* = 8, 4.6%; postnatal: *n* = 8, 2.9%), and VH with BPC (fetal: *n* = 24, 13.9%; postnatal: *n* = 15, 5.5%). The original diagnosis was updated/re-classified in 96 (21.5%) cases (fetal: *n* = 42, 24%; postnatal: *n* = 54, 19%) on the basis of our revised DWM criteria. There were no discrepancies identified in the updated diagnosis using our consensus criteria, and all diagnoses were equally misdiagnosed. Ventricular shunts were present in 43/273 (15.7%) postnatal examinations: Forty of 43 (93%) had DWM, 2 had VH, and 1 had VH with BPC. One hundred ten (23.1%) patients were found to have a genetic anomaly or abnormality; however, genetic information was available in only a minority of cases.

Most of the analyzed variables were found to be significant differentiators of DWM from non-DWM both prenatally and

postnatally (Online Supplemental Data). Posterior fossa perimeter and evidence of prior vascular injury were not significant differentiators of DWM and non-DWM phenotypes prenatally or postnatally (Online Supplemental Data). Superior posterior fossa angle, torcular location, and VH differentiated groups postnatally but not prenatally.

In the postnatal cohort, using TVA alone to differentiate patients with DWM from those without DWM resulted in a concordance (C) statistic of 0.901 (Online Supplemental Data). A linear model using TVA and patient age resulted in C-statistics of 0.901 (prenatally) and 0.925 (postnatally) for differentiating DWM and non-DWM (Online Supplemental Data). Optimized linear models generated with the stepwise Akaike information criterion resulted in C-statistics of 0.927 (prenatally) and 0.944 (postnatally) for differentiating DWM and non-DWM (Online Supplemental Data). The Akaike information criterion–optimized prenatal linear model included age, TVA, fastigial angle, and VH. The Akaike information criterion–optimized postnatal linear model included age, TVA, and fastigial angle.

Brainstem dysmorphism was found in 66.9% ($n = 220$) of children with DWM in comparison with 60.7% ($n = 71$) of children in the non-DWM group. Of the 220 children with DWM and brainstem abnormalities, most had pontine hypoplasia (86.0%; $n = 189$), while a minority had either a thickened pons and/or medulla (6.4%; $n = 14$) or a dysplastic, elongated brainstem (3.6%; $n = 8$). Pontine hypoplasia was also the most common phenotype present in children without DWM with brainstem abnormalities (84.5%; $n = 60$).

DISCUSSION

The literature is rife with confusing terminology regarding abnormalities of the posterior fossa. Imprecise definitions and inconsistent use of DWM and related terms (variant, continuum, spectrum), VH, inferior vermian hypoplasia, and partial caudal vermian agenesis have contributed to poor correlations between neuroimaging phenotypes and clinical outcome. Clarification would improve counseling for pregnancy planning, prognosis, and genetic work-up. In our cohort, we found evidence of this ongoing confusion and descriptive heterogeneity. If we used vermian structure, choroid plexus/tela choroidea location, and fastigial recess angles as primary diagnostic criteria, 96 of 407 (23.6%) posterior fossa malformations were originally misdiagnosed with a predominant bias of intraventricular hemorrhage and BPC ($n = 29$) and intraventricular hemorrhage ($n = 17$) instead of DWM.

Current diagnostic imaging criteria for DWM include VH with enlargement of the fourth ventricle and posterior fossa.¹ However, there is wide variability in the degree of vermian underdevelopment and posterior fossa enlargement, sometimes without correlation between the 2. Our results support this variability in that posterior fossa enlargement was not a significant differentiator between the DWM and non-DWM groups. Often, there are imaging features that approach but do not meet the full diagnostic criteria. While Dandy-Walker variant is an antiquated, poorly defined label, its intended use once served an important purpose: to indicate less pronounced phenotypes that appeared similar to a DWM proper. The problem with the term Dandy-Walker variant was not an intrinsic one; rather, it was that its

misuse in the literature left it without a clear definition and even rendered it, at times, misleading. Abandonment was necessary, leaving a descriptive void.

We are reluctant to overly emphasize the imaging appearance of these malformations for fear of overstating the importance of the imaging phenotype for prognosis and management. Ultimately, clinical outcome is the most important factor for prognosis, so there is a need for long-term longitudinal clinical follow-up to determine to what extent an imaging subclassification scheme matters, if at all. In addition, myriad causative mechanisms (postmigrational insult, infection, germline genetic abnormality, somatic mutation) must be better elucidated and understood in the context of the mechanism of normal cerebellar development. Evidence of prior vascular injury was found in a minority of our cohort but did not differentiate the DWM from the non-DWM group. Nevertheless, MR imaging sensitivity for hemorrhage detection wanes with time, and prior injury may be indiscernible on fetal MR imaging, particularly with insufficient resolution or when motion artifacts are present.

To fully appreciate the developmental pathogenesis of any brain malformation, one must identify the approximate timing of the insult following which development goes awry. DWM is characterized by upward, under-rotation of a hypoplastic vermis vis-à-vis the brainstem. Extensive analysis points to the posterior vermis being disproportionately hypoplastic.^{10,11} Our updated imaging criteria stem from an improved understanding of the mechanism of injury (disrupted growth of the posterior vermis) during a specific developmental epoch generally thought to result in the Dandy-Walker phenotype—that is, inferior vermian–predominant hypoplasia with an unpaired caudal lobule, an obtuse fastigial recess, a large TVA, and inferolateral displacement of the taenia-tela choroidea complex and choroid plexus, the latter due to failed resolution of the anterior membranous area.

Fourth ventricular size, posterior fossa size, and torcular location are poor imaging criteria for DWM because they are largely related to the degree of fourth ventricular outflow impedance and are not direct sequelae of the injury or malformation. Rather, imaging determination should hinge on the appearance of the vermis, choroid plexus, and tela choroidea in accordance with the time that the abnormality developed. Our receiver operating characteristic analysis quantitatively demonstrates the robust distinction between DWM and non-DWM cases with C-statistics of >0.9 when evaluating structures such as the fastigial recess or measuring the TVA. As objective measures of the more subjective DWM imaging features, these strongly predictive quantitative data may facilitate neuroimaging classification by those with less clinical expertise than our expert panel or by, yet developed, artificial intelligence tools. Although more complex linear models were more predictive (Online Supplemental Data), the strong predictive value of TVA alone suggests that such complexity may be unnecessary in most cases; however, it would be necessary to compare patients with posterior fossa abnormalities to a cohort of healthy control subjects to better determine the importance of predictive imaging variables for diagnosis.

Histopathologically, DWM is thought to be underpinned by disruption in the structure of the rhombic lip (RL), a stem cell zone located in the posterior cerebellum that gives rise to ~80% of

all neurons in the human brain, including all glutamatergic neurons in the cerebellum.^{10,11} During embryonic development, the human RL is trigonal but later expands into a tail-like structure trailing from the posterior cerebellum, with ventricular and subventricular compartments separated by a vascular bed. During this time, the fastigial recess remains flat. With an increase in size of the posterior cerebellum brought about by the outward growth of the nodulus beginning at 14 postconceptional weeks, the tail-like RL becomes integrated into the posterior-most lobule, causing the fastigial recess to sharpen (>14 postconceptional weeks).^{10,11} In comparisons of DWM and VH, it is evident that in DWM, the fastigial angle remains flat or obtuse, while in VH, the angle becomes acute. This finding provides us with some clues to the potential timing of the insult and leads to the hypothesis that in DWM, RL disruption occurs before RL internalization, while in VH, aberrations in RL development and other processes occur following internalization. The delay in RL disruption leading to restricted hypoplasia of the posterior-most lobule suggests that the early RL likely contributes to the growth of the entire cerebellum, but post-internalization helps in the growth and maintenance of the posterior lobe only. Hence, the extent of hypoplasia would depend on the timing of the RL insult, with further work required to define this developmental stage.

The concomitant presence of brainstem dysmorphism in children with abnormalities of cerebellar development is unsurprising, given that the cerebellum is a dorsal derivative of the anterior hindbrain, rhombomere 1.^{19,20} Developmentally, the neurons of the pontine nuclei arise from the both the cerebellar RL in rhombomere 1 and the RL of other more posterior hindbrain rhombomeres. These neurons migrate tangentially to their final position in rhombomeres 3 and 4.^{19,20} Because both DWM and VH exhibit similar and statistically indistinguishable rates of pontine hypoplasia, this feature suggests that the pontine hypoplasia seen in these conditions is most likely due to a combination of deficient pontine nuclear neurogenesis/histogenesis and WM fiber reduction commensurate with the degree of cerebellar hypoplasia.

The growth and development of the posterior vermis are the most protracted of all regions, making it especially vulnerable to disruptive events.^{10,11,21} The inferior vermis is the most common and most severely involved region in DWM and isolated vermian hypogenesis, ie, partial agenesis.¹¹ Nonetheless, inferior VH should be diagnosed only if it can be documented that the inferior vermis is small. Otherwise, the more general term “vermian hypoplasia” should be used.²¹ “Hypoplasia” should be reserved for a small but otherwise structurally normal-for-age vermis.²² The other less discussed and appreciated fact is that in some circumstances, one or more of these diagnoses may be present, further hampering interpretation (eg, VH and Blake pouch anomalies). Larger Blake pouch anomalies cause vermian measurement inaccuracies,⁶ thereby making vermian height in isolation an inadequate determinant for the Dandy-Walker phenotype, as seen in our prenatal cohort. Furthermore, the TVA is variable in both DWM and BPC. Although marked TVA enlargement strongly supports the diagnosis of DWM, the opposite is not true: Mild TVA elevation may be present in either DWM or BPC.

The retrospective nature of this cohort study and imaging review is a limitation and is subject to case-selection bias. Because the bulk of the cohort was accrued from imaging reports containing the terms “Dandy-Walker” and “vermian hypoplasia,” it lacks an unknown number of cases that were missed, misinterpreted, or mislabeled by the original interpreting radiologist. It also lacks a control group. This study, although the largest reported, is only the first step toward a more complete understanding of the Dandy-Walker phenotype and its (likely numerous) etiologies and diverse clinical presentations. Future work must involve more clinical outcome data, longitudinal clinical and imaging data, histopathologic and genomic analysis, healthy controls, and prenatal clinical history if we hope to bridge the divide between imaging appearance and clinical outcome. Ultimately, we aim to better understand the causes and contributing factors that result in the Dandy-Walker phenotype, and with that mechanistic understanding, we hope that we will one day be able to predict outcomes, heritability, and the likelihood of similar abnormalities in future pregnancies.

CONCLUSIONS

Objective measures have confirmed statistically the modern phenotypic features of DWM and allow differentiation from VH and BPC, causing misclassification in nearly one-quarter of prior reports. The modern DWM phenotype is best defined by inferior, predominant VH (mandatory), inferolateral displacement of the tela choroidea/choroid plexus (mandatory when visible), an unpaired caudal lobule (mandatory when visible), an enlarged tegmento-vermian angle, and an obtuse fastigial recess, the latter 2 being the most significant qualitative measures. Posterior fossa size and torcular location should be eliminated from the diagnostic criteria. We highlight the fact that the structural phenotype, while providing some information about developmental timing, bears no relevance to the etiology, whether genetic or acquired, except in rare cases where there is evidence of prior hemorrhage, inflammation, or other injury. This refined imaging phenotype may help guide future study of the numerous etiologies and varied clinical outcomes.

ACKNOWLEDGMENTS

Biostatistician W. John Boscardin, PhD, reviewed the data and assisted with the statistical analysis.

Disclosure forms provided by the authors are available with the full text and PDF of this article at www.ajnr.org.

REFERENCES

1. Barkovich AJ, Raybaud CA. **Congenital malformations of the brain and skull.** In: Barkovich AJ, Raybaud CA, eds. *Pediatric Neuroimaging*. 6th ed. Wolters Kluwer; 2019:531
2. Wüest A, Surbek D, Wiest R, et al. **Enlarged posterior fossa on prenatal imaging: differential diagnosis, associated anomalies and postnatal outcome.** *Acta Obstet Gynecol Scand* 2017;96:837–43 [CrossRef Medline](#)
3. Lerman-Sagie T, Prayer D, Stöcklein S, et al. **Fetal cerebellar disorders.** *Handb Clin Neurol* 2018;155:3–23 [CrossRef Medline](#)

4. Nagaraj UD, Kline-Faith BM, Horn PS, et al. **Evaluation of posterior fossa biometric measurements on fetal MRI in the evaluation of Dandy-Walker continuum.** *AJNR Am J Neuroradiol* 2021;42:1716–21 [CrossRef Medline](#)
5. Aldinger KA, Timms AE, Thomson Z, et al. **Redefining the etiologic landscape of cerebellar malformations.** *Am J Hum Genet* 2019;105:606–15 [CrossRef Medline](#)
6. Whitehead MT, Vezina G, Schlatterer SD, et al. **Taenia-tela choroidea complex and choroid plexus location help distinguish Dandy-Walker malformation and Blake pouch cysts.** *Pediatr Radiol* 2021;51:1457–70 [CrossRef Medline](#)
7. Bernardo S, Vinci V, Saldari M, et al. **Dandy-Walker malformation: is the “tail sign” the key sign?** *Prenat Diagn* 2015;35:1358–64 [CrossRef Medline](#)
8. Paladini D, Donarini G, Parodi S, et al. **Hindbrain morphometry and choroid plexus position in differential diagnosis of posterior fossa cystic malformations.** *Ultrasound Obstet Gynecol* 2019;54:207–14 [CrossRef Medline](#)
9. Nelson MD, Maher K, Gilles FH. **A different approach to cysts of the posterior fossa.** *Pediatr Radiol* 2004;34:720–32 [CrossRef Medline](#)
10. Haldipur P, Aldinger KA, Bernardo S, et al. **Spaciotemporal expansion of the primary progenitor zones in the developing human cerebellum.** *Science* 2019;366:454–60 [CrossRef Medline](#)
11. Haldipur P, Bernardo S, Aldinger K, et al. **Evidence of disrupted rhombic lip development in the pathology of Dandy-Walker malformation.** *Acta Neuropathol* 2021;142:761–76 [CrossRef Medline](#)
12. Twickler DM, Reichel T, McIntire DD, et al. **Fetal central nervous system ventricle and cisterna magna measurements by magnetic resonance imaging.** *Am J Obstet Gynecol* 2002;187:927–31 [CrossRef Medline](#)
13. Chapman T, Menashe SJ, Zare M, et al. **Establishment of normative values for the fetal posterior fossa by magnetic resonance imaging.** *Prenat Diagn* 2018;38:1035–41 [CrossRef Medline](#)
14. Jandeaux C, Kuchcinski G, Ternynck C, et al. **Biometry of the cerebellar vermis and brain stem in children: MR imaging reference data from measurements in 718 children.** *AJNR Am J Neuroradiol* 2019;40:1835–41 [CrossRef Medline](#)
15. Dovjak GO, Brugger PC, Gruber GM, et al. **Prenatal assessment of cerebellar vermian lobulation: fetal MRI with 3-Tesla postmortem validation.** *Ultrasound Obstet Gynecol* 2018;52:623–30 [CrossRef Medline](#)
16. Kline-Faith B, Bulas D, Bahado-Singh R. *Fundamental and Advanced Fetal Imaging: Ultrasound and MRI.* Wolters Kluwers; 2015
17. Pertl B, Eder S, Stern C, et al. **The fetal posterior fossa on prenatal ultrasound imaging: normal longitudinal development and posterior fossa anomalies.** *Ultraschall Med* 2019;40:692–721 [CrossRef Medline](#)
18. Whitehead MT, Vezina G. **The fetal falx cerebelli.** *Pediatr Radiol* 2020;50:984–89 [CrossRef Medline](#)
19. Watson C, Bartholomaeus C, Puelles L. **Time for radical changes in brain stem nomenclature-applying the lessons from developmental gene patterns.** *Front Neuroanat* 2019;13:10 [CrossRef Medline](#)
20. Leto K, Arancillo M, Becker EB, et al. **Consensus paper: cerebellar development.** *Cerebellum* 2016;15:789–828 [CrossRef Medline](#)
21. Robinson AJ, Blaser S, Toi A, et al. **The fetal cerebellar vermis: assessment for abnormal development by ultrasonography and magnetic resonance imaging.** *Ultrasound Q* 2007;23:211–23 [CrossRef Medline](#)
22. Malingier G, Lev D, Lerman-Sagie T. **The fetal cerebellum: pitfalls in diagnosis and management.** *Prenat Diagn* 2009;29:372–80 [CrossRef Medline](#)